This article was downloaded by: [Chonbuk National University]
On: 02 August 2012, At: 04:51
Publisher: Taylor & Francis
Informa Ltd Registered in England and Wales Registered Number: 1072954 Registered office: Mortimer House, 37-41 Mortimer Street, London W1T 3JH, UK

Liquid Crystals
Publication details, including instructions for authors and subscription information:
http://www.tandfonline.com/loi/tlct20

Achieving high light efficiency and fast response time in fringe field switching mode using a liquid crystal with negative dielectric anisotropy

Hong Jun Yun [a], Mi Hyeon Jo [a], In Won Jang [a], Seung Hee Lee [a], Seon Hong Ahn [b] & Hae Jin Hur [b]

[a] Department of BIN Fusion Technology and Department of Polymer-Nano Science and Technology, Chonbuk National University, Jeonju, Jeonbuk, Korea

[b] Samsung Mobile Display Co, Cheonan, Chungnam, Korea

Version of record first published: 19 Jun 2012

To cite this article: Hong Jun Yun, Mi Hyeon Jo, In Won Jang, Seung Hee Lee, Seon Hong Ahn & Hae Jin Hur (2012): Achieving high light efficiency and fast response time in fringe field switching mode using a liquid crystal with negative dielectric anisotropy, Liquid Crystals, 39:9, 1141-1148

To link to this article: http://dx.doi.org/10.1080/02678292.2012.700078

PLEASE SCROLL DOWN FOR ARTICLE

Full terms and conditions of use: http://www.tandfonline.com/page/terms-and-conditions

This article may be used for research, teaching, and private study purposes. Any substantial or systematic reproduction, redistribution, reselling, loan, sub-licensing, systematic supply, or distribution in any form to anyone is expressly forbidden.

The publisher does not give any warranty express or implied or make any representation that the contents will be complete or accurate or up to date. The accuracy of any instructions, formulae, and drug doses should be independently verified with primary sources. The publisher shall not be liable for any loss, actions, claims, proceedings, demand, or costs or damages whatsoever or howsoever caused arising directly or indirectly in connection with or arising out of the use of this material.

Liquid Crystals,
Vol. 39, No. 9, September 2012, 1141–1148

Taylor & Francis
Taylor & Francis Group

Achieving high light efficiency and fast response time in fringe field switching mode using a liquid crystal with negative dielectric anisotropy

Hong Jun Yun[a], Mi Hyeon Jo[a], In Won Jang[a], Seung Hee Lee[a]*, Seon Hong Ahn[b] and Hae Jin Hur[b]

[a]*Department of BIN Fusion Technology and Department of Polymer-Nano Science and Technology, Chonbuk National University, Jeonju, Jeonbuk, Korea;* [b]*Samsung Mobile Display Co., Cheonan, Chungnam, Korea*

(*Received 1 May 2012; final version received 31 May 2012*)

The fringe-field switching (FFS) mode has been widely applied in high-resolution portable liquid crystal displays because of its excellent performances in transmittance, viewing angle, and operating voltage. Up to now, the FFS mode utilised a liquid crystal with positive dielectric anisotropy owing to fast response time and low operating voltage. This paper proposes a merit of using a liquid crystal with negative dielectric anisotropy. The optimised cell structures with thin cell gap and fine patterned electrode structures make the FFS mode with negative liquid crystals exhibit higher transmittance than that of the positive liquid crystals and a fast response time.

Keywords: Liquid Crystal Display; Fringe-field switching; Negative dielectric anisotropy

Downloaded by [Chonbuk National University] at 04:51 02 August 2012

1. Introduction

Nowadays, liquid crystal displays (LCDs) are widely used for all kinds of displays such as mobile phones, tablet personal computers, notebooks, monitors and televisions, etc, replacing cathode-ray tube (CRT) displays. In addition, industries pursue to develop high resolution LCDs over 300 pixels per inch(ppi) so that human eyes cannot easily distinguish the spatial distances between pixels at all, realising perfect images [1]. However, high-resolution LCDs result in serious loss of the transmittance because the number of scanning gate and signal lines are increasing with increasing resolution. The sacrifice of transmittance of the display is never favourable, especially in portable displays because it causes increase in power consumption.

In LCDs, mainly liquid crystal (LC) modes determine the performance and cost of the products [2]. At present, LCDs for mobile phones utilise several LC modes such as twisted nematic (TN) [3], polymer-stabilised vertical alignment (PS-VA) [4–6] mode, in-plane switching (IPS) [7–9] mode, and FFS mode [10–13]. However, the FFS mode has become the main mode of use for high performance and high resolution LCDs [1]. Many electro-optic studies on the FFS mode using a LC with positive dielectric anisotropy (+LC) have been reported [14–23]. According to previous studies [19, 24], the transmittance in the FFS mode is dependent on cell gap and it decreases with decreasing cell gap (d). In general, LCDs show relatively slower response time of ~ms than that of the emissive displays. Since the decaying response time is proportional to d^2, lowering d is prerequisite to achieve a fast response time. However, such an approach decreases transmittance further and this technological barrier needs to be overcome. Although all present commercialised FFS-LCDs uses a +LC because of low operating voltage, and fast response time, the transmittance still needs to be improved further. Interestingly, the first commercialised FFS mode used a LC with negative dielectric anisotropy (–LC) [10]. The FFS mode with –LC shows much higher transmittance than that with +LC but it shows intrinsically higher operating voltage due to low magnitude of dielectric anisotropy and slower response time due to larger rotational viscosity than that with +LC. This paper works on how to improve transmittance as well as response time in the FFS mode with –LC.

2. Switching principle of the FFS mode and simulation conditions

In the FFS mode, regardless of whether a +LC or –LC is used, the plane shape of the common (pixel) electrode lies above the substrate and the passivation layer exists above the common electrode. The pixel (common) electrode exists in a slit form above the passivation layer with the pixel electrode width (w) and distance (l) between them, as shown in Figure 1.

Both electrodes are made of transparent materials, in order to obtain a high transmittance. In the device, the LCs are homogeneously aligned in the initial state and the optic axis of the LC is coincident with one of the axes of the crossed polariser. As a result, the device appears to be dark in the off state. When an electric field is generated between the pixel

*Corresponding author. Email: lsh1@chonbuk.ac.kr

ISSN 0267-8292 print/ISSN 1366-5855 online
© 2012 Taylor & Francis
http://dx.doi.org/10.1080/02678292.2012.700078
http://www.tandfonline.com

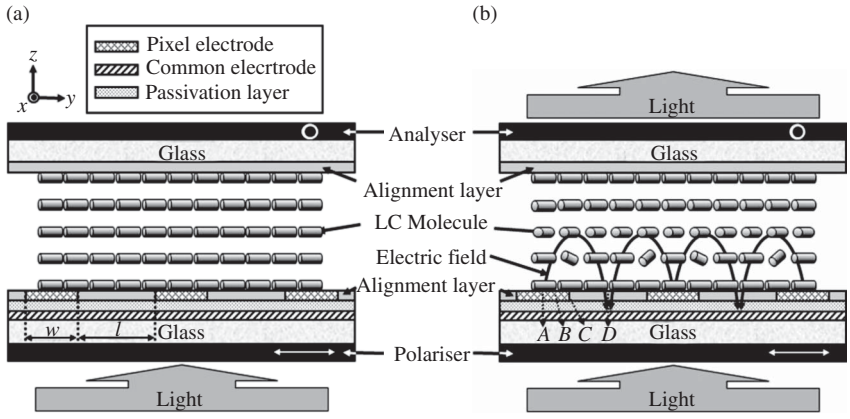

Figure 1. Schematic cell structure with molecular orientation in the FFS mode with –LC (a) off state and (b) on state.

Downloaded by [Chonbuk National University] at 04:51 02 August 2012

and common electrodes, fringe-electric fields having horizontal (E_y) and vertical (E_z) field components are generated and this field rotates the LC directors and then the transmittance is generated, as shown in Figure 1. In the device, E_y is not constant along the y direction, due to the cell structure [18], that is, it oscillates periodically and thus the transmittance also oscillates along the electrodes, because the dielectric torque required to rotate the LCs varies along the y direction. Another interesting point regarding the FFS mode is that two torques, the dielectric torque between the LC director and E_y at first and then the elastic torque between the neighbouring LC molecules rotates the LC. In this way, the LC molecules rotate above whole electrode surface but the rotating degree is not constant along the y direction, instead it changes periodically. The difference in the rotating angle Ψ causes the transmittance difference because the transmittance is proportional to $\sin^2(2\Psi)$. The reduction of the thickness of the cell gap makes the difference in transmittance along the y direction larger, reducing the overall transmittance.

In order to analyse the electro-optic characteristics of a FFS mode using a –LC, we performed a simulation using "LCD master" (Shintech, Japan), where the motion of the LC directors are based on the Eriksen-Leslie theory and the optical transmittance is calculated using a 2×2 extended Jones Matrix [25, 26]. In the calculations, the thickness of the passivation layer between the electrodes is 2900 Å. The physical properties of the –LC ($\Delta\varepsilon = -4.0$, $K_1 = 13.5$ pN, $K_2 = 6.5$ pN, $K_3 = 15.1$ pN, rotational viscosity (γ_1) was 104 mPa s) are used and the strong anchoring of the LC to the surface was assumed. The surface pre-tilt angle for both substrates is 2° and the initial alignment of the LC is 10° for the –LC with respect to the E_y of the fringe electric field. The transmittances of the single and parallel polarisers are assumed to be 45% and 35%, respectively.

3. Results and discussion

In order to investigate voltage-dependent transmittance (V–T) curves according to cell gaps, standard electrode structures with $w = 3$ μm and $l = 4.5$ μm were chosen. The cell thickness (d) was varied from 4 μm to 2 μm and the birefringence of the LC was tuned to yield a cell retardation value of 0.36 μm at 550 nm. As shown in the V–T curves of Figure 2, the operating voltages increase from 4.6 V to 4.8 V and 5.6 V and the normalised transmittance (or light efficiency) decreases from 0.87 to 0.84 and 0.73 as the cell thickness decreases from 4.0 μm to 3.0 μm and 2.0 μm, respectively.

In other words, the transmittance-dropping ratio is about 4.0% and 16.0% when d is reduced from 4.0 μm to 3.0 μm and 2 μm, respectively. To understand this in detail, the LC orientation in a white state is calculated at four different electrode positions A, B, C, D (see Figure 1) in which A and D indicate a centre of patterned electrode and a centre between patterned electrodes, B indicates a position between the edge and the centre of the electrodes, and C indicates the position for the edge of electrodes as shown in Figure 3.

Understanding field-respondent LC orientation at these electrode positions gives enough information how the transmittance generated is associated with LC deformation on the device since the distance from A to D is a repeatable unit along the y direction. When d is 4.0 μm, the maximal twisted angle from the initial position is strongly dependent on the electrode position such that it is about 65° at $z/d = 0.2$ for position C and 48° at $z/d = 0.38$, 52° at $z/d = 0.35$, and 44°

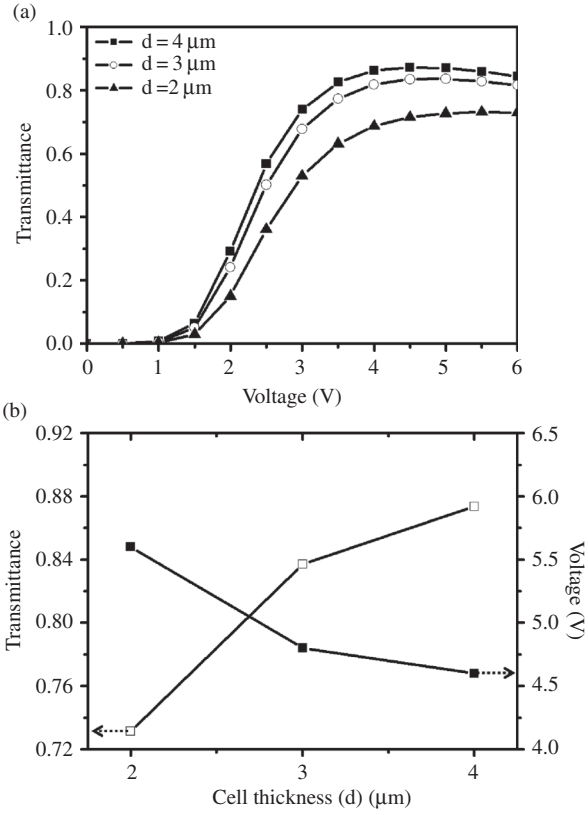

Figure 2. (a) V–T curves and (b) maximum transmittance and operating voltage as a function of cell thickness at $w = 3.0$ μm and $l = 4.5$ μm.

at $z/d = 0.40$ for position A, B, and D, respectively (see Figure 3 (a)). It is known that the light modulation follows polarisation rotation at C and phase retardation at A, B and D in the FFS mode [18]. For the phase retardation method, the transmittance becomes maximal when the effective rotation angle of LC director is 45°. When $d = 4.0$ μm, electrode positions A, B, and D show excellent transmittance given with optimised retardation of the LC layer. When d is smaller than 4.0 μm, the twist angles at electrode positions A, B, and D decreases significantly. For example, when $d = 2.0$ μm, the maximal twisted angle moves from near bottom substrate to middle of cell thickness and it is about 68° at $z/d = 0.3$ for position C. This indicates that the light modulation might be changed from the polarisation rotation effect to the phase retardation effect at position C and the LC director is twisted over maximal twist angle for highest transmittance, giving rise to transmittance less than maximum. In addition, the maximal twisted angles are 36°, 45°, and 30° at $z/d = 0.5$ for position A, B, and D, respectively (see Figure 3 (c)), indicating that the transmittance at positions A and D does not reach maximal transmittance.

When the cell gap is 3μm, the degree of transmittance is strongly dependent on electrode positions so that the average transmittance is much less than 0.8, which is not desirable for low power consumption LCDs. In order to minimise the transmittance dependence on electrode positions, various electrode structures are evaluated with varying w from 1 μm to 4 μm while keeping the l/w ratio at 1.5. According to the calculated V–T curves, the operating voltage increases rapidly when w is smaller than 2 μm and the transmittance increases with finer electrode pattern but it shows maximum at $w = 2$ μm and further finer pattern of $w =$ 1 μm, does not show further improvement, as shown in Figure 4(a).

In order to check why the device with $w = 2$ μm shows slightly better transmittance than that with $w = 3$ μm, the transmittance has been calculated along the y direction, as shown in Figure 4(b). As clearly indicated, the transmittance is oscillated according to electrode position but finer electrode pattern reduces the transmittance difference between electrode positions. Overall, the cell with fine electrode structure with $w = 2$ μm shows a slightly increased operating voltage of 4.9 V compared with 4.6 V in the cell with $w = 3$ μm but the transmittance increases from 0.87 to 0.89.

To confirm the difference in transmittance according to electrode structure, the transmittance at 550 nm is calculated by rotating the LC cell in the white state counter-clockwise under the crossed polariser, as shown in Figure 5.

When $w = 3.0$ μm, the transmittance at position A shows a repeating pattern of maximal and minimal transmittance every 45° though the minimal transmittance does not show clear extinction of the light. This indicates the optic axis of LC director at A exists whereas it does not at C. From this behaviour, we conclude that the light modulation of electrode position A is close to phase retardation whereas it is close to polarisation rotation at position C. With a finer electrode pattern of $w = 2.0$ μm, the transmittance change is similar to the previous case but the transmittance difference between minimum and maximum is reduced. This indicates that the light modulation at position A does not occur by phase retardation effect purely, instead, it becomes mixed concept of both methods in fine patterned electrode structure.

Next, how fine patterned electrode structure ($w =$ 2.0 μm and $l = 3.0$ μm) affects the V–T curves when the cell gap becomes less than 4 μm, as shown in Figure 6.

As indicated, the operating voltage is almost kept constant when the cell gap decreases from 4.0 μm to 3.0 μm, and it increases from 4.9 V to 5.1 V with further decreases to 2.0 μm. Surprisingly, the

Downloaded by [Chonbuk National University] at 04:51 02 August 2012

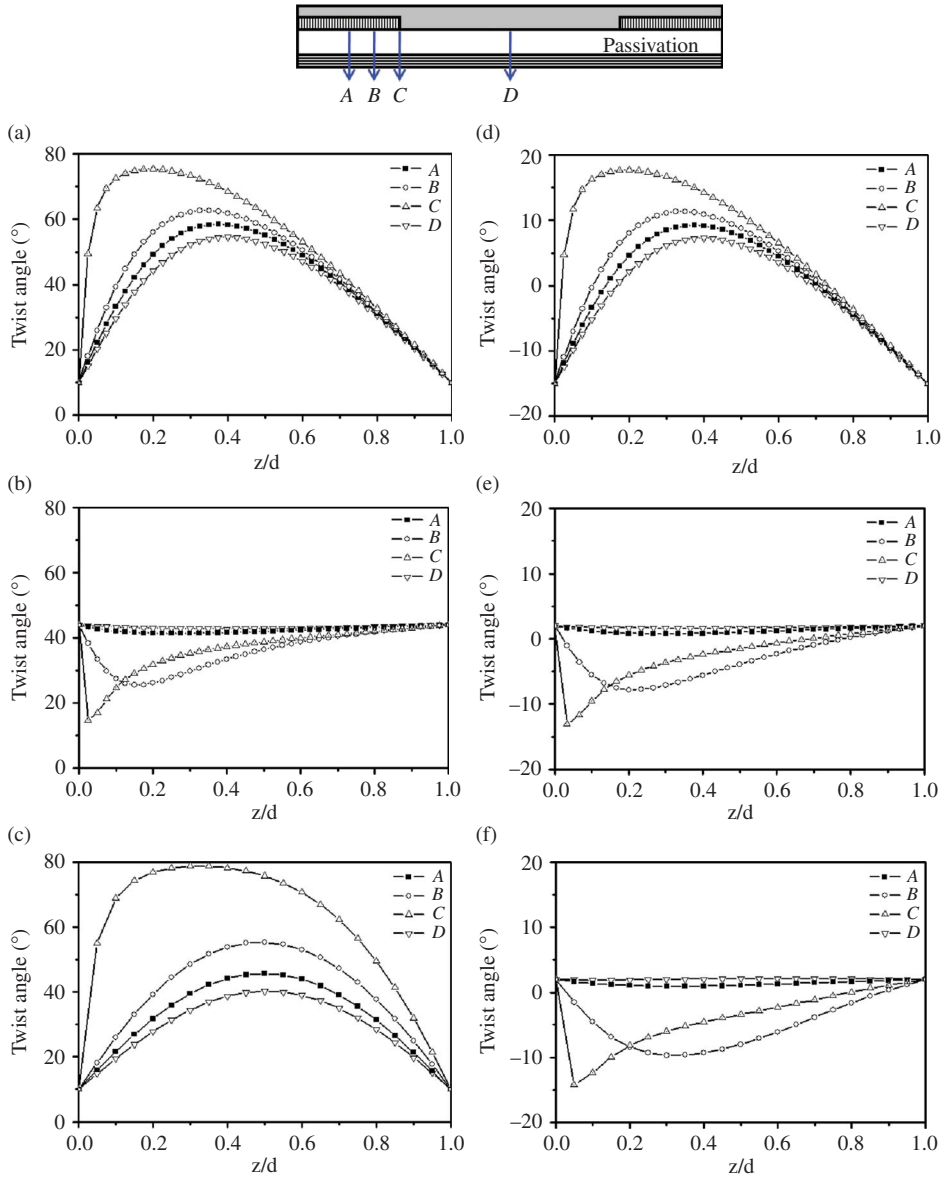

Figure 3. Director profile of twist and tilt angle at four different electrode positions; (a, d) $d = 4.0$ μm, (b, e) $d = 3.0$ μm and (c, f) $d = 2.0$ μm at $w = 3.0$ μm and $l = 4.5$ μm.

transmittance drops only about 1.2% and 6.2% though the cell gap decreases from 4.0 μm to 3.0 μm and 2.0 μm, respectively, while in the conditions of $w = 3.0$ μm and $l = 4.5$ μm, the transmittance drops about 4.2% and 16.3% as the cell gap decreases from 4.0 μm to 3.0 μm and 2.0 μm, respectively. The results clearly imply that the fine patterned electrode structure can exhibit high transmittance, and proper operating voltage and even fast response time because cell thickness can be thinned like 3 μm or less up to 2.0 μm.

Figure 7 shows how the transmittance changes with decreasing cell gap according to the electrode position for two representative electrode structures.

In the electrode structure $w = 3.0$ μm and $l = 4.5$ μm, the transmittance decreases in all areas with decreasing the cell gap and especially, it drops rapidly at electrode positions A, C, and D. On the other hand, the transmittance decreasing rate with decreasing the cell gap at the same electrode positions is reduced greatly in the electrode structure $w = 2.0$ μm and $l = 3.0$ μm, while still keeping a high transmittance over 0.84 even at low cell gap of 2.0 μm.

In order to understand the excellent electro-optic characteristics in the cell with a fine patterned electrode structure, the LC orientation in a white state was calculated at four different electrode positions when the d is 4.0 μm, 3.0 μm and 2.0 μm as shown in Figure 8.

When d is 4.0 μm, the maximal twisted angle from the initial position occurs about 65° at $z/d = 0.15$

Downloaded by [Chonbuk National University] at 04:51 02 August 2012

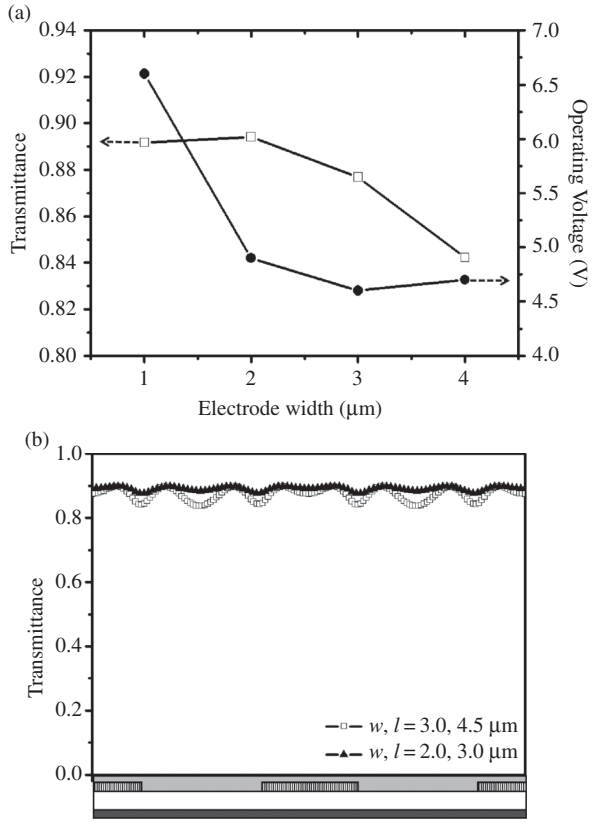

Figure 4. (a) Maximum transmittance and operating voltage and (b) electrode-position-dependent transmittance as a function of pixel electrode width and the distance between them.

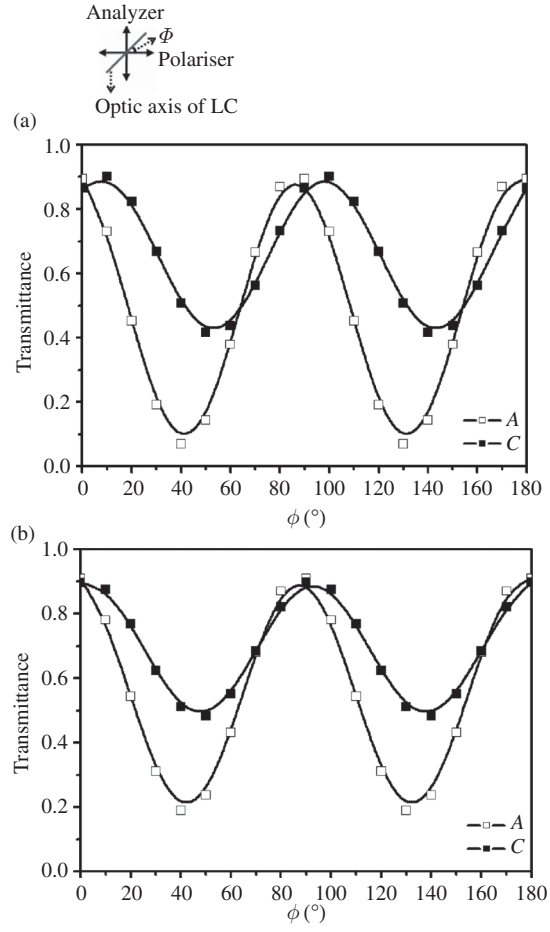

Figure 5. Transmittance as a function of the rotation angle of the crossed polariser in the white state; (a) $w = 3.0$ μm and $l = 4.5$ μm, (b) $w = 2.0$ μm and $l = 3.0$ μm.

for position C and 53°, 56°, and 51° at $z/d = 0.3$ for electrode positions A, B and D, respectively, with low tilt angles in an average of less than 1.7° (see Figure 8 (a) and 8 (d)). The LC profile indicates that the light modulation in all area is associated with the polarisation rotation effect, that is, the fine patterned electrode structure is changing the light modulation from a mixed concept of polarisation rotation and phase rotation effects to a polarisation rotation effect in most areas (see Figure 3). When d is 3.0 μm, the maximal twisted angle is strongly dependent on the electrode position such that it is about 64° at $z/d = 0.2$ for position C and 49°, 53°, and 47° at $z/d = 0.33$ for position A, B, and D, respectively (see Figure 8 (b)). Since for the cell ($w = 3.0$ μm and $l = 4.5$ μm) at the same cell thickness the maximal twisted angle from the initial position is about 66° at $z/d = 0.23$ for position C and 44° at $z/d = 0.43$, 50° at $z/d = 0.4$, and 39° at $z/d = 0.46$ for position A, B, and D, respectively (see Figure 3 (b)), the twisted angles at positions A and D does not reach the effective rotating angle 45°, resulting in a much lower transmittance than that with a fine patterned cell. When d becomes very thin (2.0 μm), the effects of the fine patterned electrode are more pronounced. While the maximal twisted angles at positions A and D are 36°, and 30° at $z/d = 0.5$ for the cell ($w = 3.0$ μm and $l = 4.5$ μm), they are 42°, and 40° at $z/d = 0.4$ in the fine patterned cell, indicating that fine patterned cell shows much higher transmittance at positions A and D where the LC director is twisted by mainly elastic torque between neighbouring molecules.

Finally, the response time characteristics have been compared between two representative electrode structures ($w = 2.0$ μm and $w = 3.0$ μm) as shown in Table 1. In the FFS mode, the field induces mainly twist deformation so that the field-response behaviour of the LC director is similar to that of the IPS mode [7, 27] and the rising (τ_{on}) and decaying time (τ_{off}) is given as follows in Equations (1) and (2):

Downloaded by [Chonbuk National University] at 04:51 02 August 2012

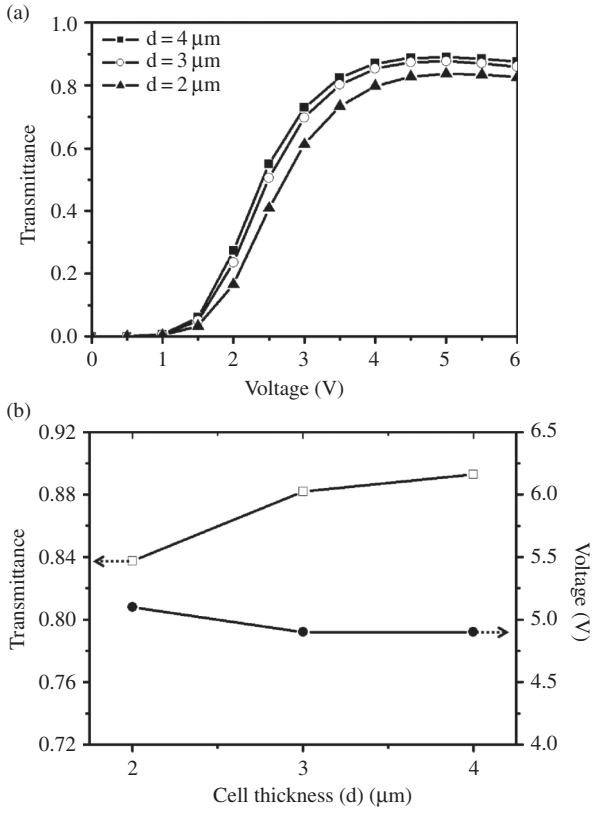

Figure 6. (a) V–T curves and (b) maximum transmittance and operating voltage as a function of cell thickness at $w = 2.0$ μm and $l = 3.0$ μm.

$$\tau_{on} = \frac{\gamma d^2}{\pi^2 K_{eff}\{(V^2 - V_{th}^2) - 1\}} \quad (1)$$

$$\tau_{off} = \frac{\gamma d^2}{\pi^2 K_{eff}} \quad (2)$$

Since we have kept all the physical properties of the LCs the same for the two electrode structures, the difference in the response time comes purely from electrode structure effects. As indicated, both τ_{on} and τ_{off} become much faster to less than 10 ms in both electrode structures. Especially in the fine patterned cell with $w = 2.0$ μm, the cell gap effects on reduction of response time is much clear because the electric field is relatively more localised near the electrode surface than that with $w = 3.0$ μm.

4. Summary

In order to achieve very high transmittance in the FFS mode for super high-resolution displays, a LC with negative dielectric anisotropy was investigated. In general, the LC with negative dielectric anisotropy has a higher rotational viscosity than that of a LC with positive dielectric anisotropy, resulting in a slow response time. Our studies show that the FFS cell with a fine patterned electrode structure and electrode width of 2.0 μm and thin cell gaps of less than 3.0 μm can show high light efficiency over 0.8 as well as fast response times while keeping a proper operating voltage. We believe that the FFS mode using a LC with negative dielectric anisotropy is highly suitable for high performance and high-resolution FFS-LCDs.

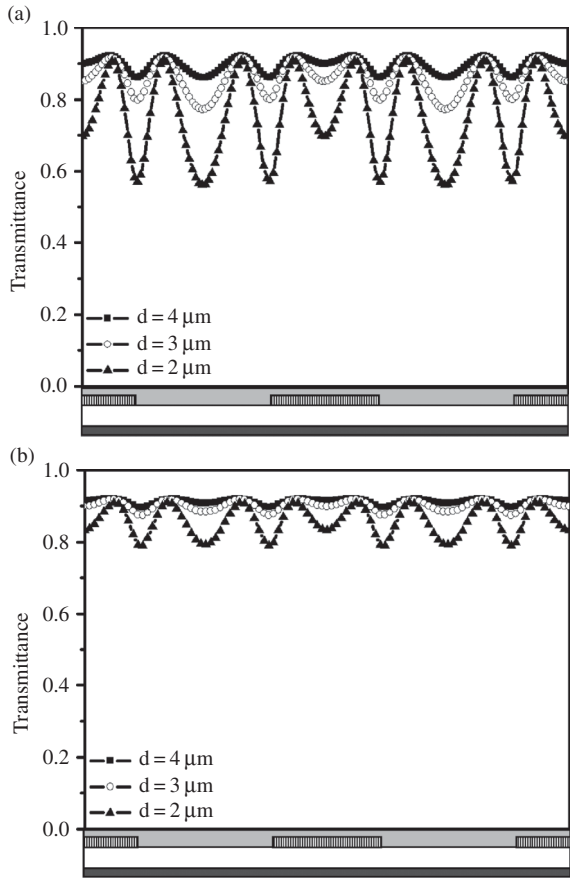

Figure 7. Electrode-position-dependent transmittance as function of cell gap (a) $w = 3.0$ μm and $l = 4.5$ μm, (b) $w = 2.0$ μm and $l = 3.0$ μm.

Acknowledgements

This study was supported by the World Class University program (R31-20029) funded by the Ministry of Education, Science and Technology and also by Samsung Mobile Display Corporation.

Downloaded by [Chonbuk National University] at 04:51 02 August 2012

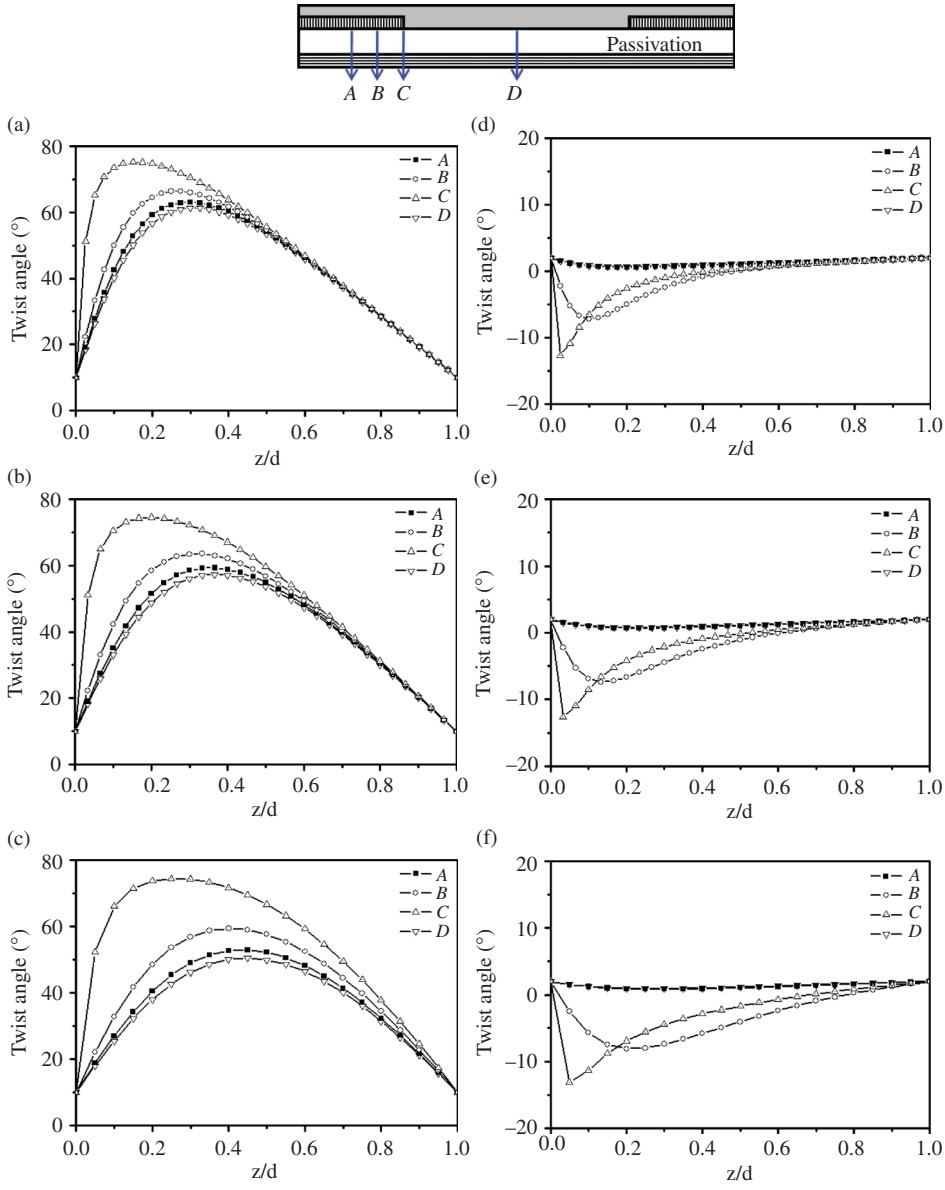

Figure 8. Director profile of twist and tilt angle at four different electrode positions; (a, d) $d = 4.0\ \mu m$, (b, e) $d = 3.0\ \mu m$ and (c, f) $d = 2.0\ \mu m$ at $w = 2.0\ \mu m$ and $l = 3.0\ \mu m$.

Table 1. Response time characteristics of the FFS mode with –LC as a function of cell gaps at two different electrode structures.

	$w = 3.0\ \mu m$ and $l = 4.5\ \mu m$		$w = 2.0\ \mu m$ and $l = 3.0\ \mu m$	
Cell gap (μm)	τ_{on} (ms)	τ_{off} (ms)	τ_{on} (ms)	τ_{off} (ms)
4	19	34	20	35
3	12	20	11	19
2	8	9	6	8

References

[1] Lee, S.H.; Bhattacharyya, S.S.; Jin, H.S.; Jeong, K.-U. *J. Mater. Chem.* **2012**, *22*, 11893–11903.

[2] Lee, S.H.; Hong, S.H.; Kim, J.M.; Kim, H.Y.; Lee, J.Y. *J. Soc. Inf. Disp.* **2001**, *9*, 155–160.

[3] Schadt, M.; Helfrich, W. *Appl. Phys. Lett*. **1971**, *18*, 127–128.

[4] Hanaoka, K.; Nakanishi, Y.; Inoue, Y.; Tanuma, S.; Koike, Y. *SID Int. Symp. Dig. Tech. Pap.* **2004**, *35*, 1200–1203.

[5] Kim, S.G.; Kim, S.M.; Kim, Y.S.; Lee, H.K.; Lee, S.H.; Lee, G.-D.; Lyu, J.-J.; Kim, K.H. *Appl. Phys. Lett.* **2007**, *90*, 261910–261919.

Downloaded by [Chonbuk National University] at 04:51 02 August 2012

[6] Lee, S.H.; Kim, S.M.; Wu, S.-T. *J. Soc. Inf. Disp.* **2009**, *17*, 551–559.
[7] Oh-E, M.; Kondo, K. *Appl. Phys. Lett.* **1995**, *67*, 3895–3897.
[8] Oh-e, M.; Kondo, K. *Jpn. J. Appl. Phys.* **1997**, *36*, 6798–6803.
[9] Jung, B.S.; Baik, I.S.; Song, I.S.; Lee, G.D.; Lee, S.H. *Liq. Cryst.* **2006**, *33*, 1077–1082.
[10] Lee, S.H.; Lee, S.L.; Kim, H.Y. *Appl. Phys. Lett.* **1998**, *73*, 2881–2883.
[11] Lee, S.H.; Lee, S.L.; Kim, H.Y.; Eom, T.Y. *SID Int. Symp. Dig. Tech. Pap.* **1999**, *30*, 202–205.
[12] Lee, S.H.; Lee, S.M.; Kim, H.Y.; Kim, J.M.; Hong, S.H.; Jeong, Y.H.; Park, C.H.; Choi, Y.J.; Lee, J.Y.; Koh, J.W.; Park, H.S. *SID Int. Symp. Dig. Tech. Pap*. **2001**, *32*, 484–487.
[13] Lee, S.H.; Kim, H.Y.; Lee, S.M.; Hong, S.H.; Kim, J.M.; Koh, J.W.; Lee, J.Y.; Park, H.S. *J. Soc. Inf. Disp*. **2002**, *10*, 224–227.
[14] Lee, S.H.; Lee, S.L.; Kim, H.Y.; Eom, T.Y. *J. Kor. Phys. Soc*. **1999**, *35*, S1111–S1114.
[15] Hong, S.H.; Park, I.C.; Kim, H.Y.; Lee, S.H. *Jpn. J. Appl. Phys.* **2000**, *39*, L527–L530.
[16] Kim, H.Y.; Nam, S.H.; Lee, S.H. *Jpn. J. Appl. Phys.* **2003**, *42*, 2752–2755.
[17] Kim, H.Y.; Hong, S.H.; Rhee, J.M.; Lee, S.H. *Liq. Cryst*. **2003**, *30*, 1285–1292.
[18] Jung, S.H.; Kim, H.Y.; Kim, J.H.; Nam, S.H.; Lee, S.H. *Jpn. J. Appl. Phys.* **2004**, *43*, 1028–1031.
[19] Kim, S.J.; Kim, H.Y.; Lee, S.H.; Lee, Y.K.; Park, K.C.; Jang, J. *Jpn. J. Appl. Phys.* **2005**, *44*, 6581–6586.
[20] Kim, M.S.; Seen, S.M.; Jeong, Y.H.; Kim, H.Y.; Kim, S.Y.; Lim, Y.J.; Lee, S.H. *Jpn. J. Appl. Phys.* **2005**, *44*, 6698–6700.
[21] Lim, Y.J.; Lee, M.H.; Lee, G.D.; Jang, W.G.; Lee, S.H. *J. Phys. D: Appl. Phys*. **2007**, *40*, 2759–2764.
[22] Kim, M.S.; Seen, S.M.; Lee, S.H. *Appl. Phys. Lett*. **2007**, *90*, 133511–133513.
[23] Ryu, J.W.; Lee, J.Y.; Kim, H.Y.; Park, J.W.; Lee, G.D.; Lee, S.H. *Liq. Cryst.* **2008**, *35*, 407–411.
[24] Jung, S.H.; Kim, H.Y.; Lee, M.H.; Rhee, J.M.; Lee, S.H. *Liq. Cryst.* **2005**, *32*, 267–275.
[25] Lien, A. *Appl. Phys. Lett*. **1990**, *57*, 2767–2769.
[26] Ge, Z.; Zhu, X.; Wu, T.X.; Wu, S.T. *J. Opt. Soc. Am.* **2005**, *A22*, 966–977.
[27] Hong, S.H..; Park, I.C.; Kim, H.Y.; Lee, S.H. *Jpn. J. Appl. Phys.* **2000**, *39*, L527–L530.

Downloaded by [Chonbuk National University] at 04:51 02 August 2012